Mice Expressing a Mutant Desmosomal Cadherin Exhibit Abnormalities in Desmosomes, Proliferation, and Epidermal Differentiation

Elizabeth Allen, Qian-Chun Yu, and Elaine Fuchs

Howard Hughes Medical Institute, Department of Molecular Genetics and Cell Biology, University of Chicago, Chicago, Illinois 60637

Abstract. Desmogleins are members of the cadherin superfamily which form the core of desmosomes. In vitro studies indicate that the cytoplasmic domain of desmogleins associates with plakoglobin; however, little is known about the role of this domain in desmosome recognition or assembly in vivo, or about the possible relation of desmoglein mutations to epidermal differentiation and disease. To address these questions we used transgenic mouse technology to produce an NH_2-terminally truncated desmoglein (Pemphigus Vulgaris Antigen or Dsg3) in cells known to express its wild-type counterpart. Within 2 d, newborn transgenic animals displayed swelling of their paws, flakiness on their back, and blackening of the tail tip. When analyzed histologically and ultrastructurally, widening of intercellular spaces and disruption of desmosomes were especially striking in the paws and tail. Desmosomes were reduced dramatically in number and were smaller and often peculiar in structure. Immunofluorescence and immunoelectron microscopy revealed no major abnormalities in localization of hemidesmosomal components, but desmosomal components organized aberrantly, resulting in a loss of ultrastructure within the plaque. In regions where desmosome loss was prevalent but where some adhesive structures persisted, the epidermis was thickened, with a marked increase in spinous and stratum corneum layers, variability in granular layer thickness, and parakeratosis in some regions. Intriguingly, a dramatic increase in cell proliferation was also observed concomitant with biochemical changes, including alterations in integrin expression, known to be associated with hyperproliferation. An inflammatory response was also detected in some skin regions. Collectively, these findings demonstrate that a mutation in a desmoglein can perturb epidermal cell–cell adhesion, triggering a cascade of changes in the skin.

Epidermal cells have two major types of homophilic, cell–cell adhesion junctions: one is mediated by classical cadherins, primarily E-cadherin, and the other is mediated by desmosomal cadherins, including desmocollins and desmogleins (Hynes, 1992; Garrod, 1993; Schmidt et al., 1994). Whereas reductions in E-cadherins have been associated with various forms of epithelial cancers (Takeichi, 1993; Birchmeier and Behrens, 1994), autoantibodies to the extracellular portions of desmogleins 1 and 3, respectively, have been associated with the pathogenesis of the autoimmune disorders, Pemphigus Foliaceus, and Pemphigus Vulgaris (Stanley, 1993). It has not yet been established whether mutations in desmogleins 1 or 3 can elicit some or all of the pathological features associated with these disorders, including disruption of desmosomes, acantholysis, and in some cases, eosinophilic abscesses.

All cadherins have tripartate functional domains: (*1*) a calcium-inducible, extracellular amino-terminal domain, important for homophilic intercellular associations; (*2*) a single transmembrane-spanning domain; and (*3*) a cytoplasmic domain that anchors the cytoskeleton, an essential process for cell adhesion (Nagafuchi and Takeichi, 1988; Ozawa and Kemler, 1992). Whereas the cytoplasmic domain of E-cadherin links to the actin cytoskeleton, the cytoplasmic domains of desmosomal cadherins link to the intermediate filament cytoskeleton.

Desmocollins and desmogleins are coexpressed and often colocalized in all cells where desmosomes are found. The relative roles of these two cadherins in intercellular adhesion have only recently begun to be addressed. In elegant experiments by Troyanovsky et al. (1993), epithelial cancer cells expressing a recombinant connexin–desmocollin I produced a unique membrane-associated complex consisting of desmoplakin, plakoglobin, the chimeric pro-

Address all correspondence to Dr. Elaine Fuchs, Howard Hughes Medical Institute, Department of Molecular Genetics and Cell Biology, University of Chicago, 5841 S. Maryland Avenue, Room N314, Chicago, IL 60637. Tel.: (312) 702-1347. Fax: (312) 702-0141.

© The Rockefeller University Press, 0021-9525/96/06/1367/16 $2.00

tein, and the keratin filament cytoskeleton. In contrast, an analogous chimeric protein, composed of connexin and the cytoplasmic domain of desmoglein I, integrated into and disrupted endogenous desmosomes in cultured cells. Collectively, these studies suggest that the cytoplasmic tail of desmoglein I possesses information that can direct it to desmosomes, although it may not necessarily be essential in establishing the membrane–cytoskeletal connection.

Immunoprecipitation and gel overlay assays with cultured cell extracts or recombinant proteins indicate that at least one desmosomal component, plakoglobin, can interact directly with a specific segment of the desmoglein tail (Troyanovsky et al., 1993, 1994; Mathur et al., 1994; Roh and Stanley, 1995). Whether the association between desmoglein and plakoglobin exists within the actual desmosomes seems likely, but remains unknown. It is also not clear whether desmogleins are required to build a structurally functional and stable desmosome.

In the present study, we focus on the in vivo consequences of expressing an amino-terminally truncated form of a human desmoglein in the epidermis of mice. We patterned our mutation after an N-cadherin mutant, shown to disrupt cadherin-mediated adherens junctions in vitro and in vivo (Kintner, 1992; Fujimori and Takeichi, 1993; Levine et al., 1994; Hermiston and Gordon, 1995), and used the keratin 14 promoter to drive expression of our transgene. While this promoter is known to target gene expression to the basal layer of transgenic mouse epidermis, stable transgene products expressed by this promoter often persist in the lower spinous layers (Vassar et al., 1989).

Of the three epidermal desmogleins, Dsg2 is globally expressed in nonepidermal tissues and Dsg1 is restricted to the uppermost layers of the epidermis; only Dsg3 is known to be expressed in the basal and lower spinous layers of the epidermis and other tissues in which K14 is expressed (Arnemann et al., 1993; see also Stanley, 1993; Schmidt et al., 1994). We focused on Dsg3, not only because its expression pattern is most likely to mimic that of the transgene, but also because it is the Pemphigus Vulgaris Antigen (PVA)[1], and patients with this severe blistering autoimmune disease produce antibodies against this protein (Amagai et al., 1991; Stanley, 1993). Therefore, a Dsg3 study was likely to have significant clinical, as well as biological implications.

We show that a truncated Dsg3, Dsg3ΔN, elicits perturbations in desmosomes, accompanied by gross changes in the organization and differentiation of epidermal cells. In addition, a marked increase in cell proliferation is elicited in areas where cell adhesion is not completely lost. In regions where adhesion is lost entirely, there are pyknotic nuclei and signs of keratinocyte degeneration. Finally, marked edema and an inflammatory response is seen in the paw skin of transgenic neonatal mice. We discuss the significance of these and additional findings in relation to Pemphigus Vulgaris and other epidermal diseases, and in relation to possible functions for Dsg3 and the proteins with which Dsg3 associates.

1. *Abbreviations used in this paper*: BrdU, bromodeoxyuridine; NGS, normal goat serum; PPK, palmoplantar keratoderma; PVA, Pemphigus Vulgaris Antigen.

Materials and Methods

Construction of the Expression Vector and Generation of Transgenic Mice

Human Dsg3 (PVA) cDNAs were cloned from a human epidermis 5′ stretch cDNA library (Clontech, Palo Alto, CA) by using primers derived from the published sequence (Amagai et al., 1991). The full-length cDNA was assembled from three overlapping clones and from a small PCR product encompassing nucleotides 65–289.

To remove nucleotides 295–1790, encoding amino acid residues 72–569, a PCR mutagenesis strategy was used. A chimeric primer was made that contained nucleotides 276–294 of the Dsg3 coding sequence, directly followed by nucleotides 1791–1809. Using PFU polymerase, a PCR product was generated using this and a second 5′ primer encompassing nucleotides 65–87, resulting in a "loop-out" deletion of the desired sequences. The PCR product was purified and used as a primer in another round of amplification, this time with a second PCR primer encompassing nucleotides 1959–1979. This product was ligated to the 3′ sequence of Dsg3, and finally, the Flag epitope tag was inserted at nucleotide 288, downstream of the signal peptide and the propeptide processing sequences of the mature protein. Sequencing was used to verify the identity and fidelity of the Dsg3 sequence and the cloning steps. The truncated Dsg3, referred to as Dsg3ΔN, was then subcloned into the K14 expression vector and introduced into the germline of CD-1 mice as described previously (Vassar et al., 1989).

Immunofluorescence and Immunohistochemistry

Frozen sections of tissues were subjected to double indirect immunofluorescence. Sections of paraffin-embedded tissues were preblocked with 20% normal goat serum (NGS) and subjected to immunogold histochemistry using primary antibodies in 1% NGS (see Vassar et al., 1989). The following primary antibodies were used: rabbit anti-plakoglobin (a gift from Dr. Jacqueline Papkoff, Sugen Inc., Redwood City, CA); rabbit anti-K6 (a gift from Dr. Dennis Roop, Baylor University, Houston, TX); rabbit anti-filaggrin (a gift from Dr. Beverly Dale, University of Washington, Seattle, WA); rabbit anti-desmocollin (a gift from Dr. David Garrod, University of Manchester, England); mouse anti-Flag (M2; IBI Corp., New Haven, CT); mouse anti-desmoglein (DG3.1; American Research Products, Belmont, MA); rat anti-E cadherin (Zymed Laboratories, San Francisco, CA); rat anti-β1 integrin (Pharmagen, San Diego, CA); rabbit anti-K14 (Vassar et al., 1989); rabbit anti-loricrin (Fuchs, E., K. Turksen, and L. Milstone, unpublished data); rabbit anti-desmoplakin (Kouklis et al., 1994). HRP- and fluorescence-conjugated secondary antibodies were obtained from Jackson ImmunoResearch Laboratories (West Grove, PA), and auro probe goat anti–rabbit antiserum was obtained from Amersham Life Sciences (Arlington Heights, IL).

Ultrastructural Analysis

For regular EM, tissues were fixed in 2.5% glutaraldehyde in 0.1 M phosphate buffer and postfixed in 1.5% osmium tetroxide. The specimens were processed and stained on grids with uranyl acetate and lead citrate and examined with an electron microscope (100 CX; JOEL, USA, Inc., Peabody, MA) at 80 kv. For immunoEM, tissues were embedded in Lowicryl 4M as described previously (Coulombe et al., 1991). Rabbit polyclonal antisera used were: anti-plakoglobin, anti-desmoplakin, and anti–E-cadherin (a gift from Dr. W. James Nelson, Stanford University, Palo Alto, CA).

Results

Generation of the Transgene and Production of Mice Expressing Dsg3ΔN

As discussed above, an NH_2-terminally truncated form of a desmoglein was a good candidate for (*a*) assessing the consequences of disrupting desmosomes in vivo, and (*b*) assessing the potential relevance of desmoglein mutations to human disease. Therefore, we engineered the transgene construct shown in Fig. 1 *A*. We preserved the peptide

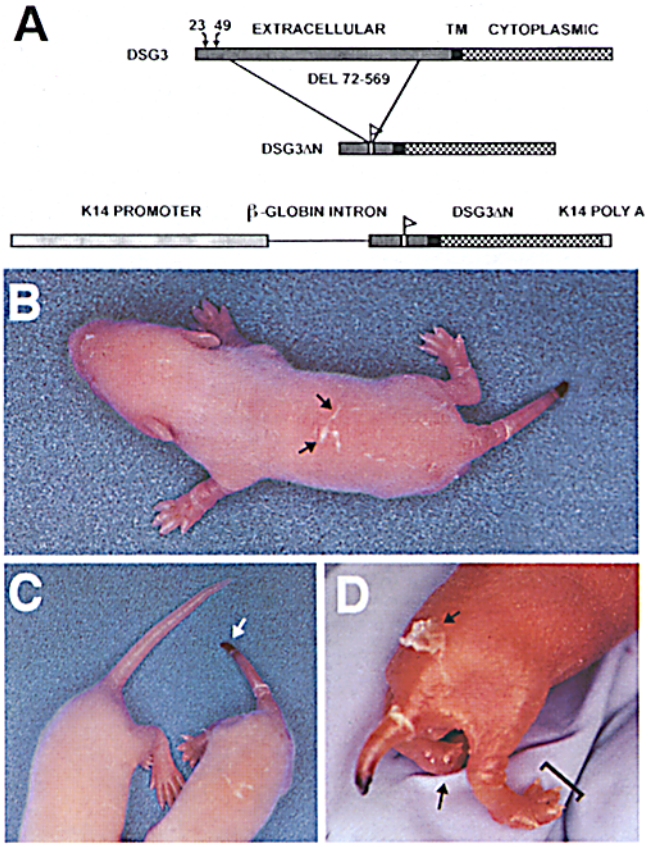

Figure 1. Transgene construct and phenotype of neonatal mice. (*A*) Dsg3ΔN transgene construct. The vector is pBluescript KS+. The components of this plasmid are the 5′ upstream sequence of the human K14 gene (Vassar et al., 1989) extending from the translation initiation codon and 5′ untranslated sequence to a HindIII site located ~2.1 kb 5′ to the TATA box, a rabbit β-globin intron, sequences encoding the leader peptide of human Dsg3 and additional amino-terminal sequence (*black stippled boxes*), sequences encoding the FLAG epitope tag (*flag*), sequences encoding the transmembrane domain (*black box*), entire cytoplasmic tail of human Dsg3 (*black dotted box*), and the K14 polyadenylation sequence (*white box*). (*B–D*) Phenotype of 5–6-d-old mice expressing Dsg3ΔN. Note the flakiness of their skin (*upper arrow* in *D* and *arrows* in *B*) and also the blackened tail of each transgenic mouse. The tails developed blackening by ~2 d of age (*arrow* in *C*, compare with control littermate's tail on the left), and tails became progressively shorter until as adults, they were only stubs. Note also the swellings of the paws, a consistent feature of 2–7-d-old transgenic mice (*D*; *lower arrow and bracket*).

leader and processing sequence for proper surface assembly of the molecule, and we added an epitope FLAG sequence just after the processing sequence so that we could monitor expression and localization of the protein. This left a small segment of the extracellular domain and the entire transmembrane and cytoplasmic domains of Dsg3 intact. As judged by immunofluorescence of transfected cultured cells, the transgene product had the ability to localize to the plasma membrane (data not shown). Additional data supportive of this notion are provided below.

Mice expressing Dsg3ΔN were produced using an outbred strain (CD-1) as described previously (Vassar et al., 1989). Seven mice were transgenic as judged by PCR analysis of their skin DNAs. Of these, two independently derived transgenic animals were bred separately to generate two lines of F1 offspring. One of the founder animals was mosaic, and gave rise to a mixture of positive and negative offspring. All F1 offspring that carried the transgene displayed phenotypic abnormalities that were inheritable. Since the two lines exhibited similar phenotypes, the aberrations were attributed to transgene expression rather than transgene integration sites. Collectively, these data indicated that expression of Dsg3ΔN had deleterious consequences for the animals.

There were three peculiarities characteristic of all affected, neonatal F1 transgenic mice (Fig. 1, *B–D*). First, within 2 d after birth, the animals developed swollen paws and digits. Second, the animals often had flaky skin, which was particularly prominent on the dorsolateral surface of the back. Finally, the tip of each transgenic mouse tail became blackened, followed by a progressive amputation of the tail as the animal aged. Adult animals had a mere stub for a tail.

To verify that the aberrant phenotype correlated with transgene expression, we isolated RNAs from the skins of 4-d-old F1 mice, and subjected them to Northern blot analysis with radiolabeled human Dsg3 (test) and actin (control) cDNAs (Fig. 2 *A*). Using the human Dsg3 probe, we detected a hybridizing band in RNAs from transgenic animals but not from control mice. The size of the major band (1.8 kb) corresponded to the expected size of transgene RNA.

To test for production of intact Dsg3ΔN, we extracted skin proteins and resolved them by electrophoresis through 9% SDS polyacrylamide gels. As judged by immunoblot analysis, samples from aberrant F1 mice contained a single 65-kD Dsg3ΔN band displaying antigenic crossreactivity with anti-FLAG antiserum (Fig. 2 *B*). This was within the range predicted for Dsg3ΔN, given the potential for glycosylation on the remaining extracellular portion of the mutant protein. Immunoblot analysis was also conducted with an anti–bovine desmoglein antibody, DG3.10, whose epitope has been mapped to the cytoplasmic repeating unit domains, present 5, 6, and 2 × in Dsg1, Dsg2, and Dsg3, respectively, i.e., the three epidermal desmogleins (Schmelz et al., 1986; Koch et al., 1990; Schafer et al., 1994). The strong 130-kD band present in all samples corresponded to the endogenous desmogleins, which are heavily glycosylated and therefore much larger than their predicted sequences (Schmidt et al., 1994). Upon longer exposure, a significantly fainter 65-kD band was seen only in protein preparations from affected and not unaffected mice (not shown). This band corresponded to the migration of Dsg3ΔN, and was judged to be less than 20 × the intensity of the 130-kD band. Since the antigenic repeats only share 50–80% sequence identity across human isotypes, and since none of the mouse desmogleins have thus far been characterized, it was not possible for us to use this antibody to compare the levels of human Dsg3ΔN with endogenous mouse desmogleins. This said, no transgene band was detected in Coomassie blue–stained SDS-PAGE gels, providing further evidence that the expression level of the transgene product was low.

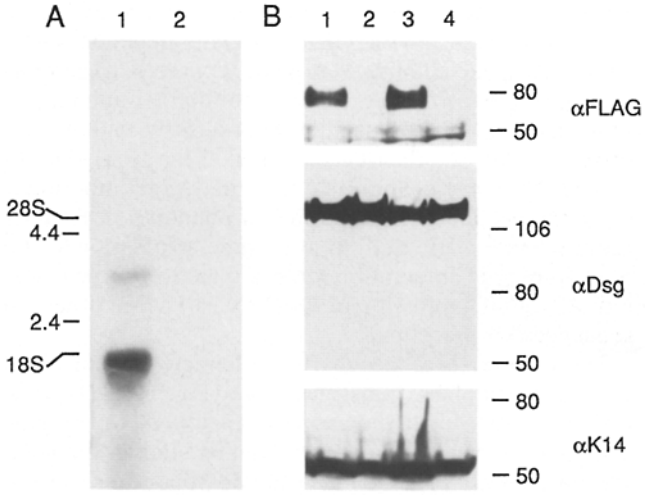

Figure 2. Dsg3ΔN mRNA and protein expression in transgenic mice. (*A*) Northern blot analysis. RNAs were extracted from the backskins of 4-d-old transgenic and control animals as described previously (Vassar et al., 1989), except for the use of Trizol reagent (Gibco BRL, Gaithersburg, MD). RNAs (15 μg each) were then resolved by electrophoresis through formaldehyde agarose gels and transferred to nitrocellulose paper. Blots were hybridized with radiolabeled cRNA probes against (*a*) nucleotide residues 1–364 of Dsg3ΔN cDNA, to test for transgene expression (shown) and (*b*) mouse actin cRNA to control for the level and integrity of the RNAs (not shown). RNAs are from: lane *1*, F1 mouse of transgenic line 1; lane *2*, control littermate of transgenic line 1. Migration of 18S and 28S rRNAs are indicated at left, along with size standards (in kb). Size of transgenic RNA was 1.8 kb, and migrated as predicted. (*B*) Immunoblot analyses. Backskin epidermis from 4-d-old animals was quick frozen, pulverized, and resuspended in 8 M urea, 10% β-mercaptoethanol, and phenyl methyl sulfonyl fluoride. After brief sonication, residual insoluble material was removed by centrifugation. Total skin extracts were then resolved by electrophoresis through 9% SDS polyacrylamide gels, which were then transferred to nitrocellulose paper by electroblotting. The blot was prestained with Ponceau red to assess that the loadings were equivalent (not shown), and then sequentially probed, stripped, and reprobed with αFLAG antibody (*top*), αDsg antibody (*middle*), and αK14 antibody (*bottom*), and developed using the chemiluminescence system (ECL; Amersham Corp.). For all blots, skin samples are from the following F1 mice: lane *1*, transgenic from line 2; lane *2*, control littermate from line 2; lane *3*, transgenic from line 1; lane *4*, control littermate from line 1. Molecular mass standards are indicated in kD at right. As expected, the Dsg3ΔN transgene product migrated as a single protein of 65 kD, analogous to that also seen in Dsg3ΔN-transfected COS cell extracts (not shown). Note: all desmogleins, comigrating at ~130 kD, cross-react with the pan anti-desmoglein mouse monoclonal antibody, DG 3.10, raised against bovine muzzle desmogleins (American Research Products, Belmont, MA). At long exposure (not shown), the transgene product could be detected with this antisera.

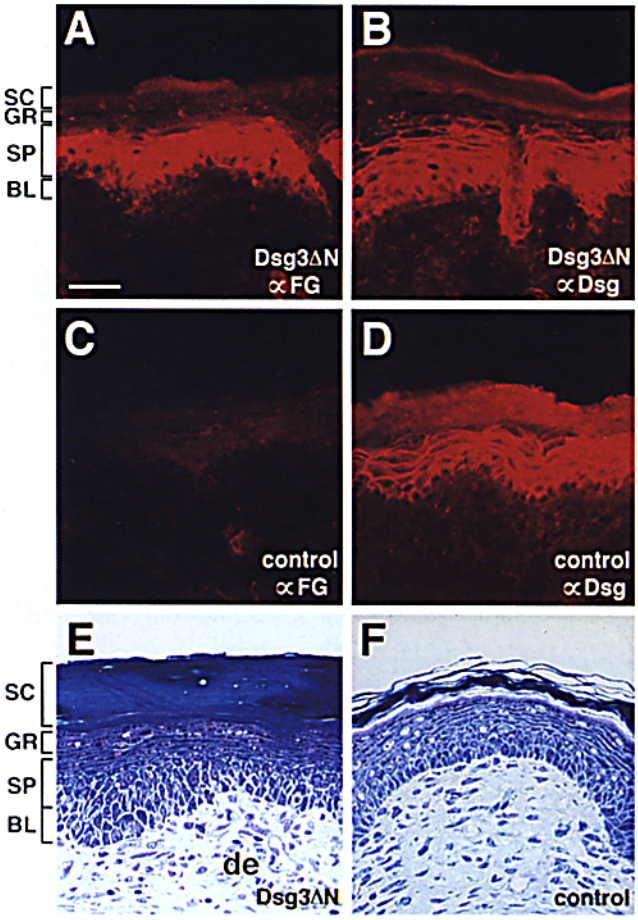

Figure 3. Expression of the transgene correlates with an increase in intercellular spaces in epidermis of Dsg3ΔN-expressing transgenic mice. (*A–D*) Paw skins from 4-d-old F1 transgenic and control animals of line 1 were frozen on dry ice for immunofluorescence. Tissues were sectioned using a Cryostat (8 μm), and processed for indirect immunofluorescence using anti-FLAG and anti-desmoglein antibodies. Immunofluorescence of transgenic (*A* and *B*) and control (*C* and *D*) skins stained with anti-FLAG (αFG; *A* and *C*) and anti-desmoglein (αDsg; *B* and *D*). Note that αFLAG staining is restricted to transgenic skin, where there is weak staining in basal layer, strong staining in lower suprabasal layers and weak or absent staining in stratum corneum. Note that αDsg staining extended more suprabasally than αFLAG. (*E* and *F*) Paw skins from 2-d-old animals were fixed and processed for semithin sectioning (0.75 μm) and staining with methylene blue. Semithin paw sections are from (*E*) transgenic line 1 and (*F*) control littermate. Note the increase in intercellular spaces in transgenic versus control epidermis. Note also the matted, thickened stratum corneum, discussed later. *de*, dermis; *BL*, basal layer; *SP*, spinous layers; *GR*, granular layers; *SC*, stratum corneum. Bar, 40 μm.

Dsg3ΔN Expression in the Epidermis Occurs in a Pattern Similar to that of Endogenous Dsg3, and Elicits Marked Changes in Intercellular Spaces within the Basal and Lower Spinous Layers

To examine the localization of Dsg3ΔN in the epidermis of trangenic animals, we used immunohistochemistry with an anti-FLAG antibody (Fig. 3). Dsg3ΔN protein was detected in the basal and lower spinous layers of the epidermis of transgenic mouse paw (*A*). The cells displaying FLAG immunofluorescence were a subset of those that showed staining with an anti-desmoglein pan antibody (*B*). The selective presence of anti-desmoglein staining in the uppermost suprabasal layers was consistent with the knowledge that Dsg1 is a late marker of epidermal differentiation. Anti-desmoglein is also known to stain Dsg2 in the basal layer of the epidermis (Schmelz et al., 1986), although the intensity of staining in this layer was not appreciably different betweeen anti-FLAG and anti-desmo-

glein. Overall, the pattern of αFLAG staining in paw skin was similar to that seen when antisera from PV patients were used to stain sections from human or mouse skin (Karpati et al., 1993; Shimizu et al., 1995, and references therein). In transgenic backskin, staining appeared weaker overall and was more prominent in the basal layer (data not shown).

We next assessed whether expression of Dsg3ΔN resulted in changes in the intercellular separations within transgenic mouse epidermis. Semithin sections of palmar skin from the paws of 2-d-old animals revealed notable separations among basal and lower spinous cells of transgenic but not control skin (Fig. 3, *E* and *F*, respectively). A number of additional morphological abnormalities were seen, and these will be discussed later. The separations within epidermis were most notable in paw and tail skin, but were also apparent in backskin. These separations were only visible in neonatal skin; within 10 d after birth, this difference could no longer be detected.

Aberrations in the Localization of Some Desmosomal Proteins in Epidermal Cells Expressing Dsg3ΔN

As judged by immunofluorescence, the anti-desmoglein staining of basal and lower spinous cells seemed somewhat more diffuse in some areas of transgenic epidermis than in control epidermis (Fig. 3, compare *B* and *D*). Even though in most cases, the staining was still predominantly peripheral, in some cases, labeling appeared to extend into the cytoplasm. This diffuse anti-desmoglein staining was not present in the upper layers of transgenic skin, where Dsg3ΔN was not present (*B*). Thus, to some extent, it seemed to correlate with expression of Dsg3ΔN. However, we show later that the regions such as paw skin, where we saw considerable diffuseness, correlated with regions that often were hyperproliferative, and therefore likely to be undergoing changes in desmosome assembly. When taken together with the dependency of the diffuseness on transgene expression, these data suggested the possibility that desmosome assembly may be somewhat altered in transgenic epidermal cells.

The distribution of other desmosomal products was also altered in some areas of Dsg3ΔN-expressing cells (Fig. 4). Thus, for example, antibodies against plakoglobin showed some cytoplasmic as well as peripheral labeling in Dsg3ΔN-expressing cells (*A–C*). Occasionally, cytoplasmic aggregates were seen which stained with anti-plakoglobin antibody (*arrows*, *B* and *D*), and also with anti-desmoglein and anti-FLAG (*arrow*, *A*). Again, in the upper layers where Dsg3ΔN was not present, anti-plakoglobin labeling was strictly peripheral (Tx red negative in *C*). The pattern of anti-desmocollin staining was also similar to that of anti-Dsg3ΔN and anti-plakoglobin (*I*, control; *J* and *K*, transgenic), although anti-desmocollin did not colocalize in cytoplasmic aggregates. As for anti-plakoglobin, except in epidermal regions which we later showed were often hyperproliferative, the labeling was predominantly peripheral, rather than cytoplasmic.

In contrast to the somewhat altered staining of anti-plakoglobin and anti-desmocollin, anti-desmoplakin staining appeared unchanged, and remained localized at the cell borders in all regions of the epidermis (compare *F* and *G*; also compare with *H*). In this regard, it is interesting that anti-desmoplakin staining has been detected at the periphery of some cells that neither possess desmosomes nor express desmogleins (Schmelz et al., 1994), and it is known that the membrane assembly pathways are distinct for desmoplakin and desmogleins (Pasdar and Nelson, 1988; Pasdar et al., 1991). Further experiments will be necessary to examine the extent to which our findings are relevant to these observations.

We were intrigued to find that even though anti–E-cadherin staining was still predominantly at the cell periphery, it too, was more diffuse in some of the Dsg3ΔN-expressing cells than in control cells (*L* and *M*). In the paw skin, it occasionally colocalized with the transgene product in cytoplasmic aggregates. This was somewhat surprising, since the desmoglein tail segment is known to have sequences that exclusively localize to desmosomes and not to classical adherens junctions (Troyanovsky et al., 1994). However, E-cadherin perturbations could be elicited indirectly by aberrations in plakoglobin distribution, since plakoglobin is known to bind to the classical cadherins (Sacco et al., 1995, and references therein). These data suggest that the two types of intercellular junctions may be linked, either physically through their cytoskeletons, or indirectly, through plakoglobin. Additional evidence related to this issue is provided below.

Structural Defects in the Desmosomes of Dsg3ΔN-expressing Epidermis

When taken together, the intercellular separations and aberrations in anti-desmosomal antibody staining suggested that desmosomes might be perturbed in cells that expressed the Dsg3ΔN transgene. We examined this possibility more closely at the electron microscopy level (Fig. 5). By ultrastructural analysis, it was readily apparent that in many regions of 2–5-d-old transgenic skin, the desmosomes of basal and lower spinous cells were markedly reduced (*A*; compare with control in *B*). In many of these areas, the numbers of cell projections, i.e., what appear to be sites of classical cadherin-mediated adherens junctions (see below), were also reduced, leaving large intercellular gaps (*asterisks*, *A*). Despite the loss of most desmosomal structures, the few remaining cell projections and/or desmosomes were often sufficient to maintain intercellular adhesion, and only a few cells were left completely without connections. Moreover, basal cells remained firmly adherent to the basement membrane, and hemidesmosomes were of normal number and morphology. Thus, while Dsg3ΔN expression led to a marked reduction in classical desmosomes, it did not completely disrupt intercellular adhesions in our mice, nor did its effects extend to the α6β4 integrin–mediated cell substratum adherens junctions. While the extent of desmosomal perturbations varied with body region, these overall differences were seen in all skin regions.

Interestingly, there were a number of peculiar intercellular junctions in the lower spinous layers of transgenic epidermis (*C*). Some epidermal processes appeared as long zones of adhesion (*arrows*), but without the plaque-like core of desmosomes. The long adhesive processes were not observed in control epidermis, but were quite

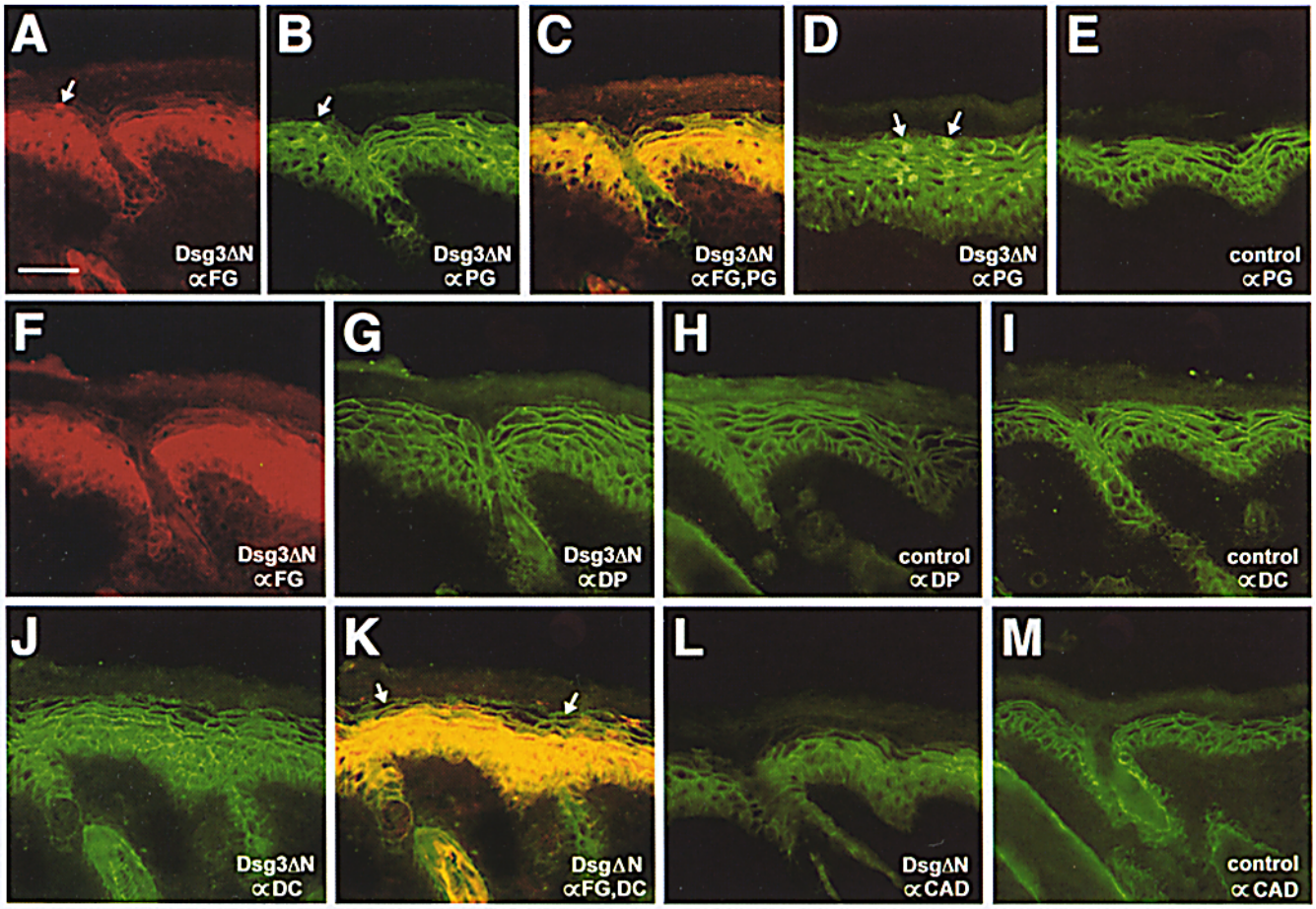

Figure 4. Aberrations in desmosomes in epidermal cells expressing Dsg3ΔN. Paw skin from 4-d-old transgenic and control animals was frozen on dry ice, and sections (8 μm) were subjected to indirect double immunofluorescence as described in Materials and Methods. (*A–D*) Transgenic skin costained with αFG (Tx red in *A*) and anti-plakoglobin (αPG; FITC in *B*). Yellow in *C* shows regions of colocalization. (*D*) Transgenic paw skin stained with αPG showing punctate cytoplasmic staining in some cells. These cells colabeled with αFG (not shown). (*E*) Control skin stained with αPG. (*F* and *G*) Transgenic skin costained with anti-desmoplakin (αDP; FITC in *G*) and αFG (Tx red in *F*). (*H*) Control skin stained with αDP. (*I*) Control skin stained with anti-desmocollin (αDC; FITC in *I*). (*J* and *K*) Transgenic skin stained with αDC (FITC in *J*) and αFG (Tx red, shown only is double label in *K*). (*L* and *M*) Transgenic (*L*) and control (*M*) skin stained with anti–E-cadherin (αCAD). Notes: both the transgene product and the desmosomal components displayed more diffuse and often cytoplasmic staining in the basal and spinous layers of regions of transgenic skin, which were later shown to be undergoing significant hyperproliferation; cytoplasmic labeling was markedly reduced in transgenic skin regions of less proliferation, and in these areas, labeling was more similar to that of control skin. Bar, 40 μm.

plentiful in transgenic epidermis. Some of these adhesion zones were associated with keratin filaments, suggesting that they contained desmosomal components, despite their atypical structure. These abnormalities will be discussed in greater depth below.

Some desmosomes were indistinguishable from wild-type. Most of these normal looking desmosomes were in the upper layers, where Dsg3ΔN did not appear to be expressed (Fig. 5, *D*, transgenic; and *E*, control). Intriguingly, some transgenic epidermal cells in the basal and spinous layers displayed atypical clumps or aggregates of keratin filaments in their cytoplasm (*F*). These filament aggregates were not in control skin. These findings suggested that the perturbations in desmosomes affected the architecture of the keratin filament network.

Given the paucity of desmosomes and their aberrant appearance, we anticipated that the organization of desmosomal components might be perturbed in the Dsg3ΔN-expressing cells. To examine this possibility, we conducted immunoelectron microscopy, using antibodies against a number of the desmosomal proteins (Fig. 6). In control cells, anti-desmocollin labeled the membrane plaque (*A* and *B*). In transgenic cells, anti-desmocollin labeling was often organized on only one side of an intercellular connection (arrows, *C*; see also inset to *C*). In addition, anti-desmocollin labeling was also seen over bundles of keratin filaments adjacent to an intercellular connection (*arrowheads* in *C* denote the connection). These data indicated that even though much of the anti-desmocollin labeling was membrane associated (except possibly for regions of epidermal hyperproliferation as in Fig. 4), the intercellular structures that it labeled were clearly aberrant.

Results with anti-plakoglobin were similar to those seen with anti-desmocollin. However, anti-plakoglobin labeling of normal desmosomes was typically arranged in rows parallel to a membrane plaque (Fig. 6 *D*). In mutant epidermis, plakoglobin was often associated with the membrane periphery, but in a disorganized fashion relative to con-

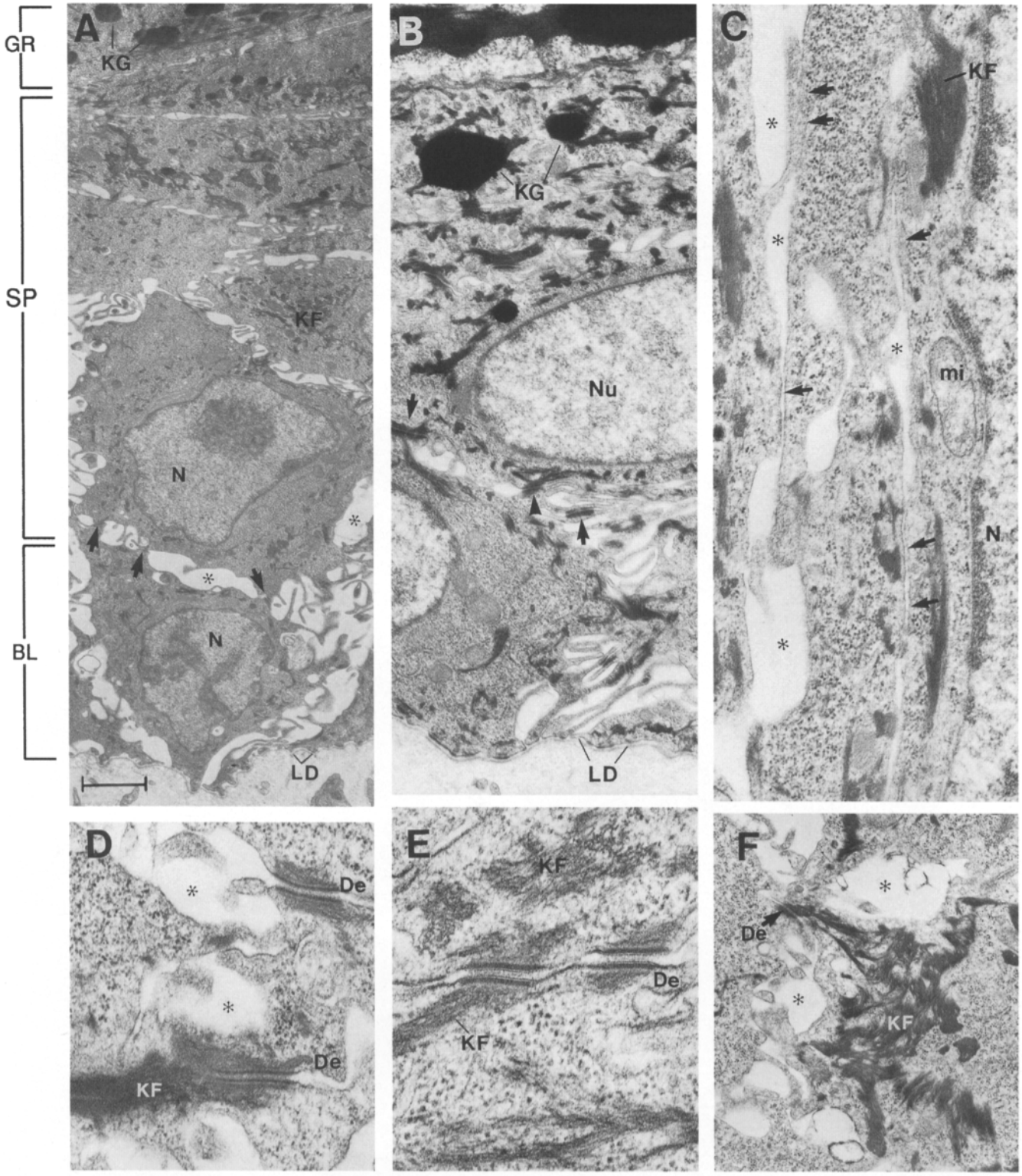

Figure 5. Aberrations in the desmosomes of basal and suprabasal epidermal keratinocytes from Dsg3ΔN-expressing transgenic mouse skin. Paw and backskins from 2–5-d-old transgenic mouse line 1 and a control littermate were fixed and sectioned for regular electron microscopy (see Materials and Methods). (*A*) Low magnification of transgenic back skin, revealing normal adherence of basal epidermal cells to the basal lamina, but gross interepidermal separations of basal and lower spinous cells. (*B*) Control skin at ×2.85 the magnification as in *A*. Note the increase in thickness of skin in transgenic relative to control. (*C*) Higher magnification revealing peculiar intercellular junctions in transgenic epidermis. Some junctions appeared as long regions of adhesion, but with no plaque-like structure (*arrows at top*); others resembled desmosomes, but sometimes lacked keratin filaments on one side of the structure (*arrows at bottom*). (*D* and *E*) Seemingly normal desmosomes in upper layers of transgenic skin (*D*) and throughout control skin (*E*; shown is cell in lower layers). (*F*) Atypical clumps or aggregates of keratin filaments in a suprabasal cell of transgenic mouse skin. These aggregates were never seen in control skin and were relatively rare in transgenic skin. They were found in regions where there was a marked paucity of desmosomes. *KG*, keratohyalin granule; *LD*, lamina densa; *Nu*, nucleus; *mi*, mitochondria; *KF*, keratin filaments; *De*, desmosome; *, intercellular space. Bar in (*A*), 1.8 μm in *A*; 630 nm in *B*; 400 nm in *C*; 200 nm in *D*; 110 nm in *E*; and 520 nm in *F*.

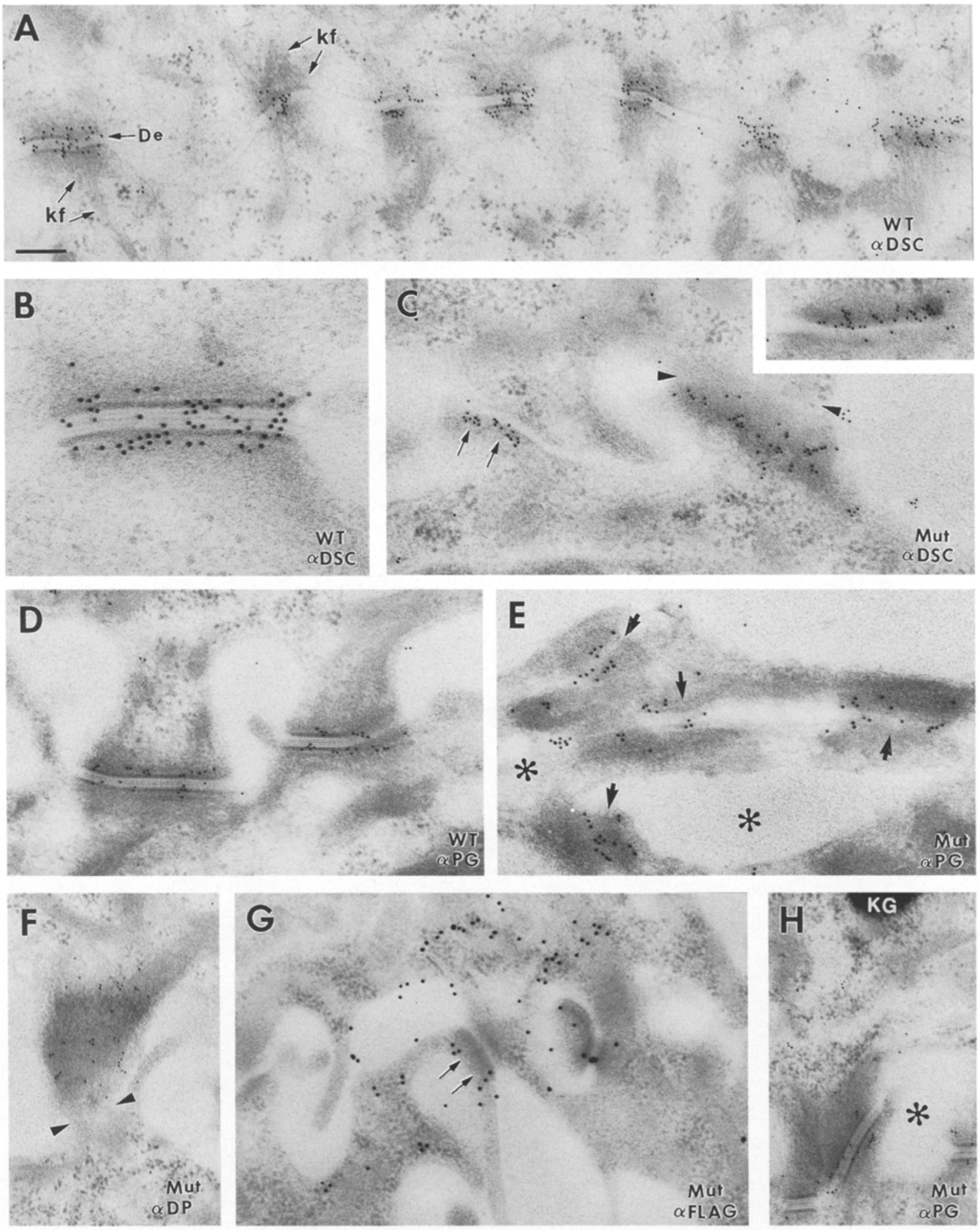

Figure 6. Aberrations in the ultrastructure of intercellular adhesion sites containing Dsg3ΔN and other desmosomal components. Paw skins from 2-d-old transgenic and control mice were fixed and processed for immunoelectron microscopy as described in Materials and Methods. Ultrathin sections of tissues were labeled with α-PG, αDSC, αDP, and αFLAG. The antibody used for labeling is indicated in the lower right of each frame, along with the source of the epidermal tissue (wild-type, WT, or DSGΔN (Mut). (*A*) Classical desmosomes connecting two basal epidermal cells. (*B*) Higher magnification of normal desmosome depicting classical plaque-like ultrastruc-

trols (*E*). In many cases, plakoglobin labeling was seen on both sides of intercellular junctions that possessed keratin filament bundles (*arrows in upper part of E*). However, as was seen for anti-desmocollin labeling, these anti-plakoglobin–labeled intercellular junctions were devoid of the ultrastructure typical of normal desmosomal cores.

Desmoplakin also labeled peculiar intercellular junctions in the transgenic basal and inner suprabasal layers (*F*). Often, desmoplakin labeling concentrated over the keratin filament bundles adjacent to the junction (example shown in *F*). This type of labeling was also seen for plakoglobin (*lower arrowhead in E*) and for desmocollin (*labeling below arrowheads in C*). Intriguingly, even when the transgenic cell labeling with these antisera was cytoplasmic, keratin filaments were often the sights of these gold particles (not shown). Collectively, these data underscore the tight association of desmosomal components with the keratin filament network.

A key question is whether the mutant desmoglein perturbed desmosomal ultrastructure by titrating out a key component, or whether it did so by physically integrating into the structure and disrupting its architecture. To further explore this issue, we repeated our immunoelectron microscopy studies this time using anti-FLAG antibodies. Fig. 6 *G* shows examples of clear labeling of aberrant desmosome-like structures. In this region anti-FLAG showed an increased level of cytoplasmic labeling relative to the other antibodies, suggesting that not all of the mutant protein was targeted to the membrane and incorporated into desmosomes. However, the amount that made it to the desmosomes appeared to be sufficient to perturb their structure. Whether the cytoplasmic FLAG labeling represented a fraction of the mutant protein in a conformation that was unable to assemble into desmosomes could not be assessed given the experiments described here.

While very few bona fide desmosomes could be identified in the Dsg3ΔN-expressing cells, those that did appear desmosome-like were often markedly shorter than normal. While electron microscopy of ultrathin sections could not be used to measure absolute lengths of desmosomes, the average length of transgenic desmosomes was significantly shorter than that of control desmosomes. Atypically short desmosomes were also seen in the upper suprabasal layers, although in these layers, longer desmosomes were also seen (Fig. 6 *H*). Wherever typical desmosomal morphology was observed, desmosomes displayed typical labeling with anti-plakoglobin (*H*).

Finally, we examined the cell–cell adherens junctions by using anti–E-cadherin and anti-plakoglobin antibodies. Control cells displayed numerous and highly organized cell projections, which labeled heavily with the antibody (Fig. 7 *A*). While these projections did not resemble intercellular adherens junctions in simple epithelia, they were sites of epidermal cell–cell contact, and they labeled strongly and highly specifically with antibodies against E-cadherin and plakoglobin. The only other anti–E-cadherin labeling seen above background in these tissue sections was located at the cell membrane at sites of noncell contact and at levels appreciably lower than that observed at projection sites. These projections are numerous and rich sources of intercellular contact in the epidermis. Thus, while anti-catenin labeling will be necessary to unequivocally resolve this point, it seems likely that these are bona fide E-cadherin-mediated adherens junctions.

In contrast to the control tissue, these projections in Dsg3ΔN-expressing cells seemed more disorganized and aberrant (Fig. 7, *arrowhead, B*). Often projections from a single cell associated (*arrow, B*). While some intercellular projections appeared unperturbed (*thick arrows, C*), the overall numbers of normally looking junctions were reduced relative to control tissue and seemed to be replaced by the peculiar junctions (*arrows, C*). These data suggested that the classical adherens junctions were altered in transgenic epidermal cells. Evidence consistent with this notion came from anti-plakoglobin labeling of these junctions in the mutant cells (*D* and *E*). In some cases, sites of intercellular contact showed little or no labeling (*D*). In other cases, only one-half of a projection site of intercellular contact labeled with the antibodies (*E*). These half-labeled junctions were reminiscent of the half-labeled desmosomal junctions that we observed in the transgenic cells.

Expression of Dsg3ΔN Elicits Dramatic Morphological Changes in Epidermal Differentiation

At the light microscopy level, striking morphological abnormalities could be seen in the architecture and differentiation of transgenic epidermis. Aberrations were in all skin regions of neonatal animals, although the morphology varied significantly throughout the transgenic epidermis. The example shown in Fig. 8 *A* is an especially affected region of the skin of the top (not palmar) side of the paw. In this and comparable areas, the epidermis was markedly and variably thickened (compare with *B*, control). The epidermis contained two to three times greater numbers of spinous layers, and the cells within these layers were disorganized. Often, the stratum corneum was thickened and matted (*A*). The granular layer was of variable thickness, sometimes reduced (Fig. 8 *A*) and sometimes increased (Fig. 3 *E*). Some regions of transgenic backskin displayed similar abnormalities (Fig. 8 *C*). Occasional eosinophilic cells,

ture, labeling with αDSC. (*C*) Transgenic basal cell showing disorganized labeling of aberrant desmosomes. Note presence of some desmosomes that show αDSC labeling on only one side of a junction (*arrows* in *C*; *inset, C*). Note also presence of bundle of keratin filaments, labeled with αDSC and located only on bottom side of a junction (*arrowheads*). (*D*) Two normal desmosomes interconnecting two lower spinous cells. Note that αPG labeling is more concentrated next to, rather than directly on, these plaques. (*E*) Transgenic intercellular connections between two lower spinous cells. Note αPG labeling at these junctions (*arrow*), despite the lack of a typical plaque-like structure. (*F*) αDP labeling of an aberrant intercellular junction (*arrowheads*), with cluster of keratin filaments that show marked labeling with αDP. (*G*) Aberrant desmosome-like structures of transgenic skin. Note labeling with αFLAG (*arrows*), indicating that the transgene product localizes to these structures. (*H*) Desmosomes in the granular layer of transgenic skin. *kf*, keratin filaments; *De*, desmosome; *, intercellular spaces; *KG*, keratohyalin granule. Bar in (*A*), 200 nm in *A*, inset to *C*, and *G*; 80 nm in *B*; 160 nm in *C* and *D*; 130 nm in *E*; 250 nm in *F* and 180 nm in *H*.

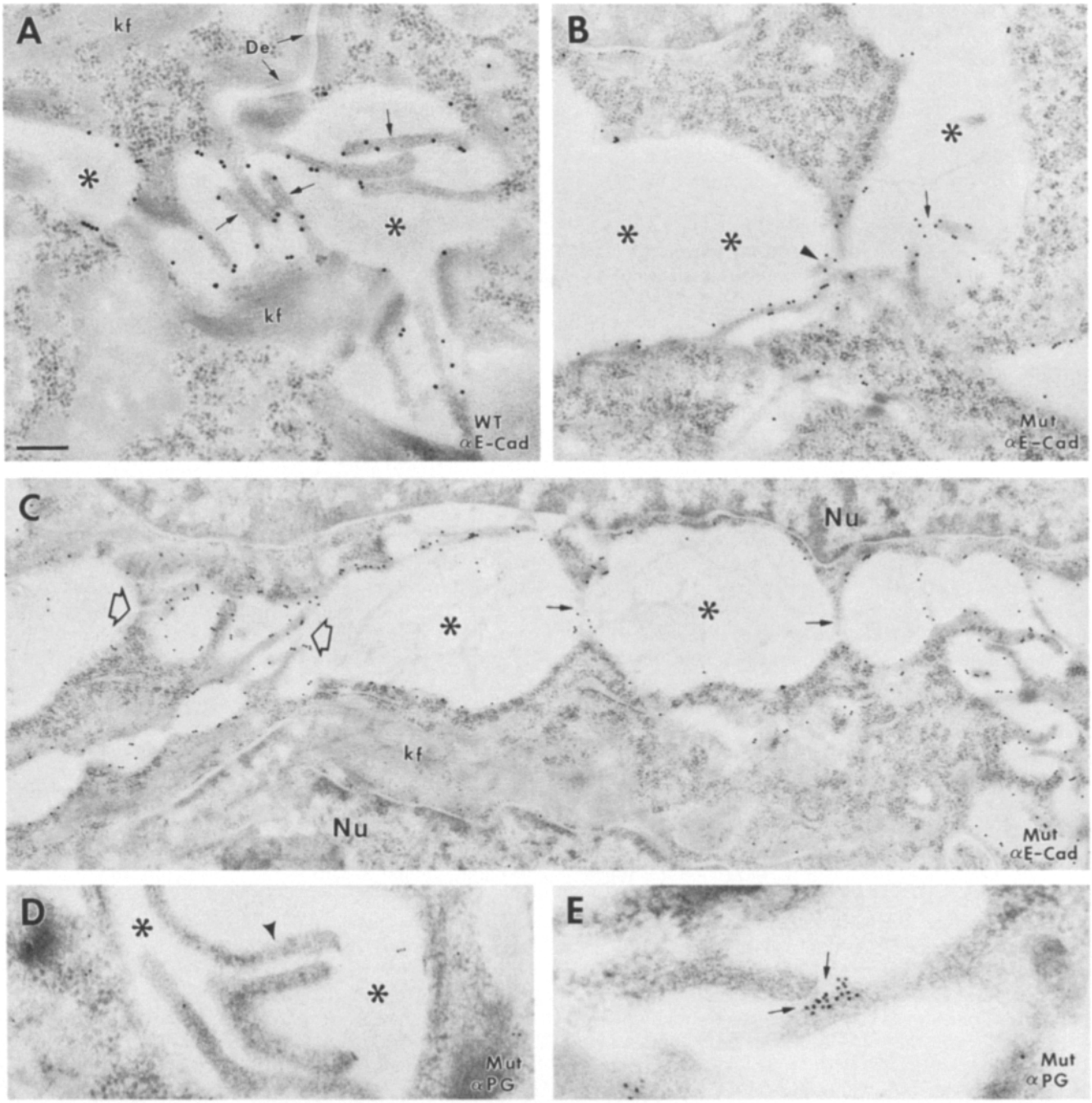

Figure 7. Aberrations in the ultrastructure of intercellular adhesion sites containing E-cadherin and plakoglobin. Paw skins from 2-d-old transgenic and control mice were fixed and processed for immunoelectron microscopy as described in Materials and Methods. Ultrathin sections of tissues were labeled with anti–E-cadherin (αCAD) and anti-plakoglobin (αPG). The antibody used for labeling is indicated in the lower right of each frame, along with the source of the epidermal tissue (wild-type, WT or DSGΔN, Mut). (*A–C*) αCAD labeling of cell–cell adherens junctions in lower spinous layers. Note the differences in regularity and uniformity of the cell projections between control and transgenic cells. Note also the wide intercellular gaps (*asterisks*) between transgenic cells. Note also the labeling along the membrane, in addition to cell to cell junctions. Note that many of the junctions are aberrant (*arrow, C*), while others are seemingly normal (*open arrowheads*). (*D* and *E*) αPG labeling of lower spinous layer adherens junctions. Note labeling of only one half of the junction in *E*, and absence of labeling in junctions in *D*. *De*, desmosome; *kf*, keratin filaments; *Nu*, nucleus; *, intercellular spaces. Bar in (*A*), 220 nm in *A*; 360 nm in *B*; 430 nm in *C*; 180 nm in *D*; and 110 nm in *E*.

signs of premature keratinocyte degeneration, were seen in the upper layers near the stratum corneum (*arrow*, *C*).

In palmar regions of paw skin, where nonbullous edema was detected, the epidermis sometimes showed pustules in the stratum corneum (*D*). These pustules contained infiltrates composed of neutrophils. The dermis underlying the affected epidermis contained both neutrophils and mononuclear cells, and was extremely watery, as judged by expansive loose and clear spaces. These were signs of an acute inflammatory response. Intriguingly, the edema and in-

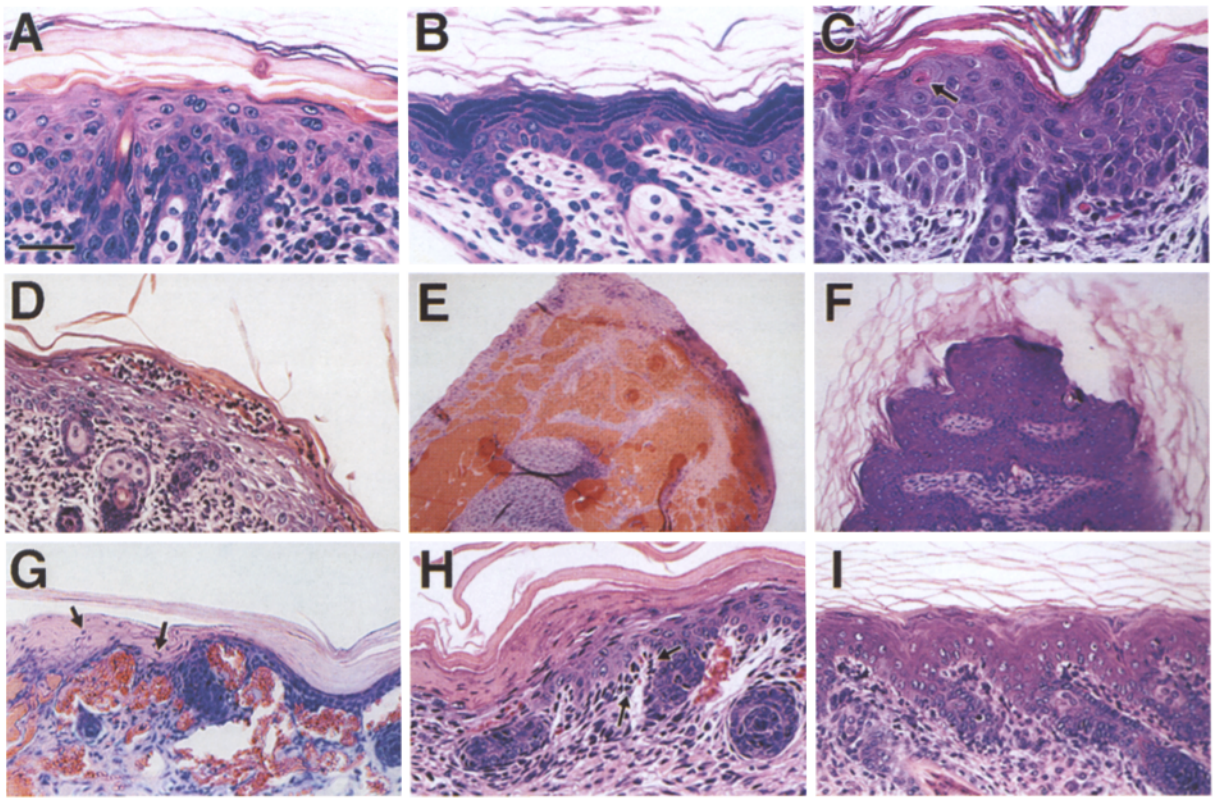

Figure 8. Alterations in tissue morphology in skin of Dsg3ΔN-expressing transgenic mice. Paw, back, and tail skins from 5-d-old F1 animals of transgenic lines 1 and 2 and their control littermates were placed in Bouin's fixative for histology. Fixed tissues from 5-d-old mice were embedded in paraffin and sectioned (5 μm). Sections were stained with hematoxylin and eosin. (*A* and *B*) Sections of transgenic and control paw skin, respectively. (*C*) Section of transgenic back skin, showing eosinophilic cell (*arrow*) in upper layer. Note: control paw skin (shown in *B*) is slightly thicker than control backskin (not shown). (*D*) Section of transgenic paw skin showing pustule and immune infiltrate in upper epidermal layers. (*E* and *F*) Low magnification of tail tips from transgenic and control skins, respectively. Note signs of degeneration, with aggregates of blood cells in transgenic tail tip. In this region, the epidermis was completely missing (*G* and *H*). Higher magnification of regions of tail skin slightly removed from the blackened epidermis. Note the presence of a matted stratum corneum and presence of nuclei (*arrows*) in the stratum corneum of *G*. This is referred to as parakeratosis. Note also the degenerative basal cells within the epidermis (*arrows*, *H*). (*I*) Control tail skin epidermis, revealing a single layer of healthy basal cells, an organized spinous, granular and stratum corneum layers, and regularly spaced hair follicles. Bar in (*A*), 30 μm in *A*, *B*, *C*, *H*, and *I*; 50 μm in *D* and *G*; 100 μm in *E* and *F*.

flammation appeared in the paws of transgenic mice at ~1–2 d after birth, and remained prominent until d 4–7 after birth, i.e., a time at which transgene expression was being reduced, as surface hairs increased in numbers. The consistency of the behavior and timing of the response made it unlikely that it was due to bacterial infection. In agreement with this notion was the absence of staining with reagents specific for gram positive and gram negative bacteria.

Additional abnormalities were prominent in the tail, where progressive self-amputation was a hallmark of these mice. Histologic examination of the tail tip revealed a complete lack of epidermis and signs of severe vascular lesions and degeneration (Fig. 8 *E*; compare with control in *F*). Further away from the tip, discernable epidermis could be identified (*G* and *H*). In these regions, abnormalities in the upper differentiating layers were striking. Often, nuclei were prevalent in the stratum corneum, a feature commonly referred to as parakeratosis (*arrows*, *G*). In addition, the statum corneum was often thicker than the rest of the epidermis. Cells in the basal layer and first few spinous layers showed severe signs of degeneration, with pyknotic, condensed nuclei surrounded by clear cytoplasm (*H*, *arrows*; compare with control in *I*). Often separations between epidermal cells appeared even greater than those shown in Fig. 3. Even in regions that were centimeters away from the tail tip, eosinophilic, degenerating keratinocytes and cell disorganization were prevalent (not shown). Whether these degenerative signs were reflective of necrosis or apoptosis remains to be explored.

In summary, throughout the epidermis of Dsg3ΔN mice, marked changes in the overall morphology occurred, and these changes extended to upper differentiating layers, despite the lack of Dsg3ΔN in these layers. We do not yet fully understand the variability either between different body sites or within regions of a particular body site; however, there did seem to be a correlation between the degree of desmosomal perturbations and the severity in aberrant differentiation. While variations in mechanical stress are likely to exacerbate regional differences, it may also be that there are as yet unexplored regional variations in patterns of desmoglein gene expression.

Expression of Dsg3ΔN Elicits Dramatic Changes in Epidermal Proliferation

The hyperthickened epidermis of the back and pawskin of Dsg3ΔN mice suggested that keratinocyte proliferation had been upregulated. To examine this possibility, we subjected 6-d-old animals to intravenous injections of bromodeoxyuridine (BrdU). 2 h later, backskins were fixed and processed for immunohistochemistry with an anti-BrdU antibody. In some regions of the epidermis, a marked increase was seen in the number of labeled cells. In regions where morphological differences were most prominent, the number of labeled cells was up to 5–8 × that of control samples (representative examples shown in Fig. 9 *A*, transgenic; and *B*, control). In control skin, all labeled keratinocytes were located as expected, i.e., in the basal epidermal layer (*arrow* in *B*), or in the outer root sheath or matrix of hair follicles. However in transgenic epidermis, some labeled cells were also in the first suprabasal layer (*A*, *arrow*), a feature typical of hyperproliferative skin disorders (for review see Potten, 1981).

The aberrations in morphology and hyperproliferation suggested that terminal differentiation might be biochemically altered in the hyperthickened areas of Dsg3ΔN-expressing epidermis. To examine this possibility, we used immunohistochemistry with antibodies against a variety of differentiation markers known to be perturbed in hyperproliferative skin disorders (Stoler et al., 1988). Most notably, antibodies against K14 revealed stronger staining in many suprabasal than basal cells (Fig. 9 *C*; compare with control in *D*). This biochemical change, also seen in psoriasis and other proliferative disorders, is known to be regulated at the mRNA level (Stoler et al., 1988), and hence may have contributed to the suprabasal Dsg3ΔN expression seen in our mice.

We also detected spinous layer expression of K6 (*E* and *F*) and β1 integrin (not shown), features typical for hyperproliferative disorders (Sun et al., 1984; Carroll et al., 1995). Moreover, the extension of anti-β1 antibody labeling into the suprabasal layers of transgenic epidermis indicated that expression of integrins could be influenced by alterations in cell adhesion, consistent with previous in vitro studies (Hodivala and Watt, 1994). Given recent findings by Carroll et al. (1995), the observation presented a possible mechanism for the hyperproliferation in our transgenic mice. Finally, in addition to changes in spinous layers, a decrease was observed in anti-filaggrin labeling (*G*; compare with control in *H*) and in loricrin labeling (*I*; compare with control in *J*). These changes were in the granular layer, where transgene expression was not observed. However, they are both changes often accompanied by hyperproliferation.

The induction of hyperproliferative markers occurred in

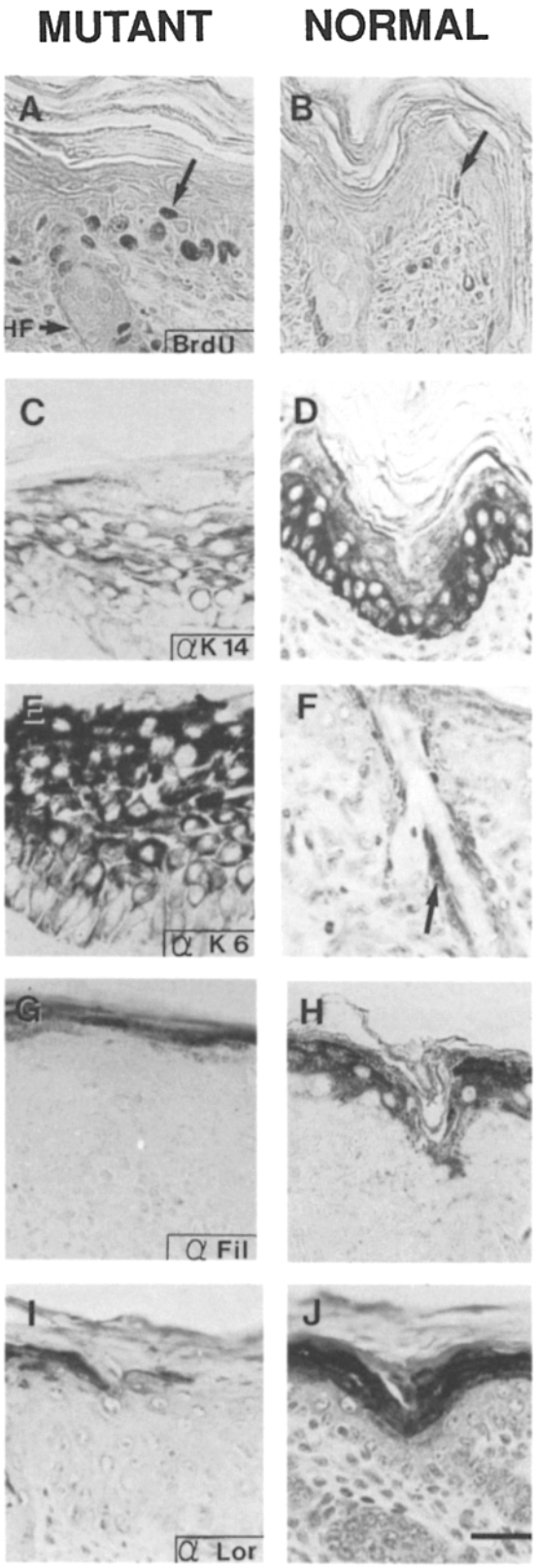

Figure 9. Hyperproliferation and altered biochemistry in the epidermis of DsgΔN transgenic mice. Five-d-old transgenic (MUT) and normal mice were injected with 100 μg BrdU in 0.8% NaCl, 1 mM Tris·HCl, pH 8.0, 0.25 mM EDTA, per gram of body weight. After 2 h, mice were killed and back and tail skins were placed in Bouin's fixative, embedded in paraffin, and sectioned (5 μm). First section of every set is transgenic; second section is control. Shown are representative sections subjected to immunogold labeling with antibodies against the following: (*A* and *B*) BrdU. Arrow in *A* denotes labeled suprabasal cell, frequently seen in transgenic skin, and never seen in control skin. (*C* and *D*) COOH-terminal peptide of mouse/human K14; (*E* and *F*) COOH-terminal peptide of mouse K6; arrow in *F* is to inner layers of outer root sheath, positive for K6. (*G* and *H*) mouse filaggrin; (*I* and *J*) COOH-terminal peptide to mouse loricrin. *HF*, hair follicle. Bar, 20 μm.

regions where an increase in BrdU labeling was also seen. However, in some body regions, e.g., the tail, degeneration was more prominent than proliferation, and BrdU labeling was nearly absent (not shown). A possible explanation for these observations is that in regions where perturbations in cell adhesion are prevalent, hyperproliferation is induced, whereas in regions where gross disruption in cell adhesion takes place, cell death ensues. While further experiments will be necessary to assess the extent to which this hypothesis is correct, our findings to date are in support of this idea.

Are There Phenotypes that Go Beyond Mere Desmosomal Disruption?

Several phenotypes in Dsg3ΔN-expressing mice were not only unexpected, but at present remain unexplained at a molecular level. Most notable was the overall appearance of adult mice (Fig. 10 *A*). Both males and females were noticeably smaller than their normal littermates. One transgenic line of F1 mice averaged 35–45% the normal weight, and the other line averaged 50–60% of the normal weight of their control littermates. Dissection revealed a marked reduction in fat pads of transgenic mice. The lack of fat was also evident in the skin, where the dermis was consequently markedly thinner than normal (*B*). In contrast to neonatal skin, the epidermis of older animals was only slightly thicker than control skin (compare *C* with *D*). Electron microscopy confirmed that a near normal complement of desmosomes was present in adult epidermis (not shown). These data are consistent with the reduction in K14 promoter activity known to occur with age (Zinkel, S., and E. Fuchs, unpublished observations). They also provide further support for the notion that a threshold level of Dsg3ΔN is necessary to produce desmosomal defects.

Another notable difference in our older transgenic mice was a constantly wet and matted hair coat, a feature particularly prominent in male animals (Fig. 10 *A*). Curiously, these animals also groomed themselves constantly, so much so that they were often on two feet rather than four. These mice also drooled, further contributing to a wet coat. It is known that the K14 promoter is active in neonatal and adult salivary glands, and that male and female glands develop differently in mice (Guo et al., 1993). Histological examination of the salivary glands revealed striking differences in both the columnar, intercalated tubular cells, which produce mucus saliva, and the alveoli, which produce watery saliva (*E*, transgenic male; compare with *F*, control). There were markedly fewer tubules in the submandibular gland of the trangenic mouse. Some of these tubules showed signs of atrophy. In those still functional, secretions were significantly more prominent than in control glands. Moreover, instead of being granular, as they were in the control, the secretory material was distinctly homogeneous in nature.

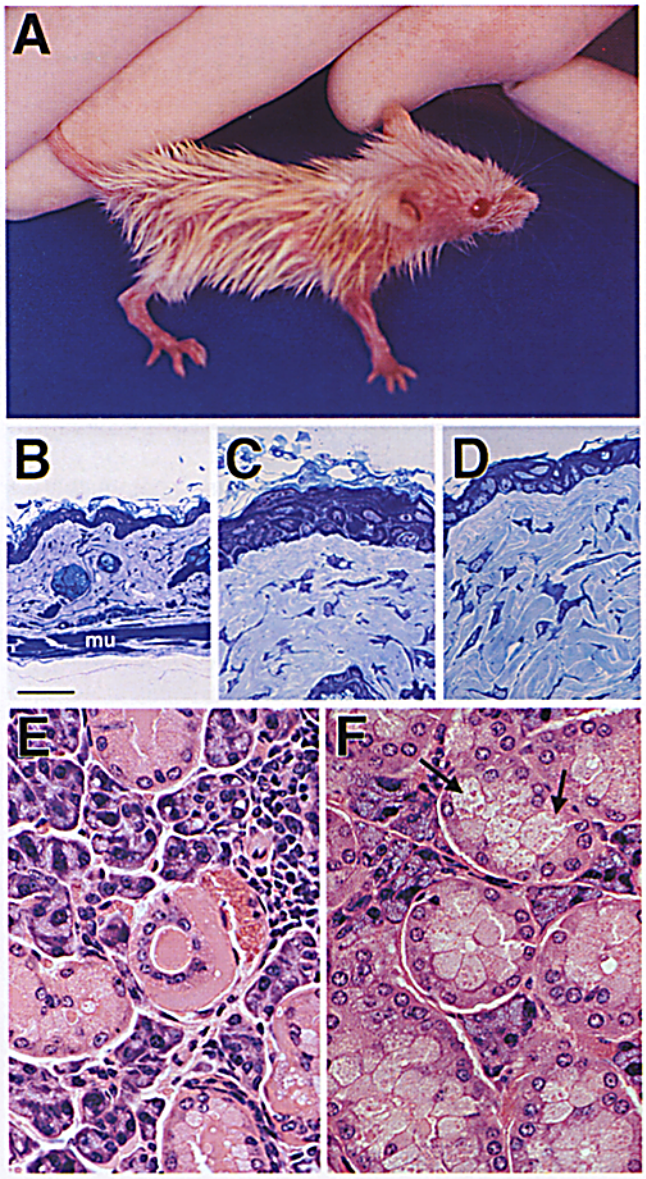

Figure 10. Adult Dsg3ΔN mice display a bizarre behavior and appearance. (*A*) A 2-mo-old animal from transgenic line 1, revealing wet and matted hair coat, due in part to virtually nonstop grooming. (*B–D*) Methylene blue–stained semithin sections of transgenic (*B* and *C*) and control backskins (*D*). Note thin dermis in *B* due to absence of skin fat. Note that transgenic epidermis of older mice is only slightly thicker than that of control. *mu*, muscle (*E* and *F*) Hematoxylin and eosin-stained sections of transgenic (*E*) and control (*F*) submandibular male salivary glands. Arrows in *F* denote granular nature of salivary solutions. In contrast, the mutant's salivary solutions were homogeneous.

Discussion

Perturbing Cell Adhesion In Vivo: What Are the Molecular Mechanisms Involved?

Our studies demonstrate unequivocally that expression of a mutant Dsg3 in epidermal cells can perturb desmosome assembly and structure in vivo, in a fashion similar to the effects of an analogous mutant N-cadherin on classical adherens junctions. Our data imply that there are two different ways in which aberrations in Dsg3 can alter human pathology: one elicited by pathogenic PVA antibodies (Amagai et al., 1992) and the other generated by genetic mutations in Dsg3.

The expression level of our transgene appeared to be low in most epidermal cells, as judged by weak desmoglein

pan antibody staining of Dsg3ΔN relative to endogenous desmogleins, and by the absence of a discernable Dsg3ΔN band in Coomassie blue–stained gels. This may explain why desmosomes were not completely lost in Dsg3ΔN transgenic mice as they are in Pemphigus Vulgaris patients. This said, the levels of Dsg3ΔN were sufficient to disrupt many of the desmosomes in the basal and lower spinous layers of neonatal epidermis. Intriguingly, despite the absence of membrane plaques with classical desmosome ultrastructure, intercellular associations still formed that labeled with antibodies against plakoglobin, desmocollin, desmoplakin, and FLAG (transgene product), and these structures associated with keratin filaments. Taken together with our regular electron microscopy data, it appears that even when the desmosome core is disrupted, thereby ablating the typical ultrastructure of the plaque, zones of adhesion containing desmosomal components can nevertheless still form. These sites of intercellular associations frequently seemed to have one-half of a plaque-like structure, suggesting that plaque disruption or perturbation need not necessarily occur on both sides of each desmosome.

It is important to consider that β-catenin and plakoglobin, homologous proteins which can associate with classical cadherins, exist in at least one and possibly more, soluble forms that have unique, as yet unidentified functions (for review see Klymkowsky and Parr, 1995). We cannot unequivocally rule out the possibility that our mutant desmoglein acted by influencing the soluble pool of plakoglobin. However, we only observed an increase in cytoplasmic plakoglobin in areas of Dsg3ΔN-expressing skin where there was extensive hyperproliferation. In these regions, cytoplasmic plakoglobin appeared to associate with Dsg3ΔN and other desmosomal components, and we speculate that this may be a reflection of an increase in the pools of desmoglein–plakoglobin preassembly complexes in hyperprolfierating epidermis. When taken together with our supposition that the levels of Dsg3ΔN are likely to be low in our transgenic mice, it seems unlikely that our mutant acted solely by interfering with putative non-adherence functions for cytoplasmic plakoglobin.

It was intriguing that in some regions of transgenic skin, cell projections were markedly reduced. Immunoelectron microscopy confirmed that these structures are involved in classical cadherin-mediated adherens junctions in the epidermis. This finding is likely to be relevant in light of the fact that in Pemphigus Vulgaris, complete loss of intercellular adhesion occurs in basal and lower spinous layers, giving rise to a "tombstone row" appearance of the cells (Lever and Schaumberg-Lever, 1990). Thus, by extrapolation, it appears that in both PV and in Dsg3ΔN transgenic mice, reduction in desmosomes leads to a reduction in E-cadherin–mediated junctions. In contrast, such a correlation did not seem to exist in A431 carcinoma cells transfected with a chimeric connexin-Dsg1 mutant (Troyanovsky et al., 1994). We cannot rule out that these differences may stem from different mechanisms of desmosome disruption in these systems, but prefer an alternative explanation, namely that when there is a reduction or alteration in desmosomes in vivo, the classical cadherin-mediated junctions are not sufficiently stable on their own to withstand the mechanical stresses of the environment. If as seems likely, the aberrant desmosomes are also sensitive to stress, then this feature, coupled with a reduction in transgene expression, could account for the overall reduction seen in histological defects as the animals developed a protective hair coat.

Relation between Disruption of Desmosomes and Changes in Cell Growth and Differentiation

An intriguing and important finding of our studies is that the perturbation in epidermal desmosomes in neonatal mice resulted in a marked increase in proliferation and hyperplasia within the epidermis. A number of possible mechanisms underlie this phenomenon. One could argue that this is caused by the concomitant reduction in classical cadherin-mediated junctions, a phenomenon that has been linked to hyperproliferation in many systems (Takeichi, 1993; Birchmeier and Behrens, 1994; Hermiston and Gordon, 1995). Alternatively, the increase in proliferation could be attributed to the observed induction of β1 integrin in the suprabasal layers, a feature associated with psoriasis, and recently shown to elicit epidermal hyperproliferation in vivo (Carroll et al., 1995). Also, it is possible that perturbation of the epidermal barrier function is the basis for induced proliferation. An ability of underlying cells to sense a defect in the overlying epidermis and respond by proliferating has been noted in epidermolytic hyperkeratosis, a degenerative disorder involving mutations in suprabasal keratins (for discussion see Fuchs et al., 1992). Loss of barrier function has also been proposed to account for elevated proliferation in other disorders (Nickoloff and Naidu, 1994). Irrespective of mechanism, the fact that a mutant desmoglein can lead to epidermal proliferation in vivo has important ramifications regarding our understanding of desmosomal functions. It presents the formal possibility that the reductions in desmosomes, often associated with patients with squamous cell carcinomas, may be an active rather than passive contributer to the enhanced proliferation seen in these tumors.

Finally, a remarkable and unexpected finding of our studies is that the expression of a mutant desmoglein elicited a myriad of morphological and biochemical changes in transgenic mice. Some of these, such as the suprabasal induction of K6 and β1 integrin, the loss of a granular layer, and the increase in thickening and parakeratosis, could be directly associated with the increase in hyperproliferation in the epidermis. However, other traits were completely unpredicted and include disorganization of cells within the epidermis, edema in palmoplantar skin, inflammatory response, formation of epidermal pustules, tail amputation, and defects in salivary glands.

Our knowledge that the mutant desmoglein leads to a reduction in cell adhesion provides explanations for some of the unusual phenomena we detected. It seems likely that when cells have reduced adherence, their outward movement towards the skin surface cannot proceed in a typically orderly fashion. In addition, while epidermal hyperproliferation seemed to be a reaction to a reduction in cell adhesion, epidermal cell death appeared to be the reaction to massive loss of cell adhesion, as occurred in the tail. In this regard, it is well known from in vitro studies that cells plated at a density which allows some cell–cell contact will proliferate, while those plated at low density

or in suspension cannot survive (see e.g., Rheinwald and Green, 1975; Frisch and Francis, 1994). Some of the other biological peculiarities of our mice are less readily explained, and remain curious enigmas. As future studies are conducted, the molecular pathways involved in these secondary responses should become more clear.

Relations between the Pathophysiologies of Dsg3ΔN Mice, Pemphigus Vulgaris, and Other Human Genetic Disorders

The loss of cell adhesion in our Dsg3ΔN mice was not as severe as that which exists in Pemphigus Vulgaris patients, where widespread acantholysis is seen in the basal and lower spinous layers (Fitzpatrick et al., 1993). In this regard, it may be relevant that C3 and other components of the complement pathway are known to be activated by pemphigus IgG (Fitzpatrick et al., 1993), and this may exacerbate the loss of cell adhesion and the blistering process in PV patients. In addition, we have discovered that despite the ability to perturb desmosomes, expression of our truncated desmoglein at low levels (and most likely a milder mutant desmoglein at much higher levels) does not obliterate cell adhesion. This finding is crucial in contemplating the types of genetic disorders that may arise from mutations in desmosomal components. Our data provide compelling evidence that desmosomes do not have to be completely disrupted in a genetic disorder involving defects in desmogleins. In fact, our data suggest that in the absence of substantial mechanical stress and with milder desmoglein mutations, it may be difficult to detect what are likely to be subtle differences in the ultrastructure of the aberrant desmosomes.

Given this finding, it is not surprising to find that Darier's disease and Hailey-Hailey's disease, two genetic disorders typified by massive loss of epidermal desmosomes, do not map to chromosome 18q where the genes for the desmogleins and desmocollins reside. Conversely, in light of our data, it is intriguing that a form of palmoplantar keratoderma (PPK) has recently been mapped near the desmosomal cadherin gene cluster (Hennies et al., 1995). The nonepidermolytic forms of this autosomal dominant group of diseases are typified by thickening of the palmoplantar epidermis and epidermal hyperplasia (Fitzpatrick et al., 1993). Interestingly, one form of nonepidermolytic PPK contains a point mutation in keratin 1 (Kimonis et al., 1994), in a region important for the association between desmoplakin and keratins in vitro (Kouklis et al., 1994). Taken together with our studies showing that the paws are the most affected areas of our animals, and that the major histopathological and/or ultrastructural features of the skin include flakiness, epidermal thickening and hyperplasia, and cytoplasmic aggregations of keratin filaments, a defect in a desmoglein could account for much of the pathology seen in the form of PPK described by Hennies et al. (1995).

As with any transgenic approach, it has been difficult to sort out the relation between the Dsg3ΔN mouse phenotype and a possible corresponding human genetic disease. Neonatal mouse and human skin are quite similar, and hence we have primarily concentrated on very young animals in drawing correlations. However unlike humans, mice quickly develop thick hair coats, and by 7–10 d, their epidermis has been concomitantly reduced to just a few cell layers. Not only does the protective hair coat make it difficult to assess mechanical stress effects on the epidermis, but in addition, the thinness of the epidermis makes it difficult to assess molecular abnormalities in the spinous and granular layers. Moreover, keeping our mice in a pathogen-free facility precludes our ability to determine the effects of epidermal barrier loss on the immune system. When taken together with the use of a keratin promoter to drive our transgene, and with a mutant which is likely to be unnaturally severe, we can only speculate as to the possible relation of our mice to human disease. Given this caveat, we have discounted some defects, e.g., salivary gland perturbations and lack of fat, on the basis of differences in transgene expression; we have discounted others, e.g., the improved adult epidermal phenotype, on the bases of transgene levels and hair coat. If these adjustments are indeed valid, the parallels between such disorders as PPK and our mice become even greater.

Certain features of other disorders are also consistent with the pathophysiology of our mice. Like PPK, nonepidermolytic variants of some other known keratin disorders are candidates for desmoglein defects. Additionally, the pathogenesis of Dsg3ΔN-expressing tail epidermis resembled to some extent that of *Pityriasis lichenoides chronica* (PLC), a cutaneous disease of unknown etiology, typified by multiple small erythrosquamous ulceronecrotic lesions (Fitzpatrick et al., 1993). Also, the pathogenesis of paw and backskin epidermis of our mice resembled that of psoriasis in some ways. This said, both PLC and psoriasis are typified by robust leukocytic infiltrates, something we did not detect in our mice. While it is not likely that they are genetic disorders of desmosomal components, some of their secondary effects may be shared with those of our Dsg3ΔN mice.

In closing, our results provide new insights into the clinical manifestations that can result from abnormalities in cell adhesion. Our studies have helped us to elucidate likely candidates for desmoglein defects, as well as to understand some of the pathophysiology of disorders that may not necessarily be directly attributable to desmosomal defects, but that are associated with abnormalities in cell adhesion.

We extend a special thank you to Ms. Linda Degenstein and Debra Dugger for their expert assistance in transgenic mouse technology and in mouse dissections and organ processing, and to Ms. M. Elizabeth Hutton for her help in cloning the cDNA for human desmoglein 3. We also thank Dr. Maria Medenica (Department of Medicine, University of Chicago), Dr. Anthony Montag (Department of Pathology, University of Chicago), Dr. Jeffrey Bluestone (Ben May Cancer Institute, University of Chicago), Dr. Len Milstone (Yale University), and Dr. Amy Paller (Children's Hospital, Chicago) for their valuable advice on the pathology of our transgenic mice. We thank Dr. James Nelson (Stanford University), Dr. Jaqueline Papkoff (Sugen Inc.), Dr. Dennis Roop (Baylor University), Dr. Beverly Dale (University of Washington), and Dr. David Garrod (University of Manchester, England), for their kind gifts of antibodies.

Dr. E. Allen was supported by a Postdoctoral Training Grant funded by the National Cancer Institute. Dr. E. Fuchs is a Howard Hughes Medical Institute Investigator. The generation of transgenic animals for this project was conducted in the transgenic facility of the University of Chicago Cancer Research Center, which receives support from the National Cancer Institute.

Received for publication 7 February 1996 and in revised form 18 March 1996.

References

Amagai, M., V. Klaus-Kovtun, and J.R. Stanley. 1991. Autoantibodies against a novel epithelial cadherin in pemphigus vulgaris, a disease of cell adhesion. *Cell.* 67:869–877.

Amagai, M., S. Karpati, R. Prussick, V. Klaus-Kovtun, and J.R. Stanley. 1992. Autoantibodies against the amino-terminal cadherin-like binding domain of pemphigus vulgaris antigen are pathogenic. *J. Clin. Invest.* 90:919–926.

Arnemann, J., K.H. Sullivan, A.I. Magee, I.A. King, and R.S. Buxton. 1993. Stratification-related expression of isoforms of the desmosomal cadherins in human epidermis. *J. Cell Sci.* 104:741–750.

Birchmeier, W., and J. Behrens. 1994. Cadherin expression in carcinomas: role in the formation of cell junctions and the prevention of invasiveness. *Biochim. Biophys. Acta.* 1198:11–26.

Carroll, J.M., M.R. Romero, and F.M. Watt. 1995. Suprabasal integrin expression in the epidermis of transgenic mice results in developmental defects and a phenotype resembling psoriasis. *Cell.* 83:957–968.

Coulombe, P.A., E.A. Hutton, A. Letai, A. Hebert, A.S. Paller, and E. Fuchs. 1991. Point mutations in human keratin 14 genes of epidermolysis bullosa simplex patients: genetic and functional analyses. *Cell.* 66:1301–1311.

Fitzpatrick, T.B., A.Z. Eisen, K. Wolff, I.M. Freedberg, and K.F. Austen, editors. 1993. Dermatology in General Medicine. 4th ed. Vol. I and II. McGraw-Hill, Inc., New York. 2979 pp.

Frisch, S.M., and H. Francis. 1994. Disruption of epithelial cell–matrix interactions induces apoptosis. *J. Cell Biol.* 124:619–626.

Fuchs, E., R.A. Esteves, and P.A. Coulombe. 1992. Transgenic mice expressing a mutant keratin 10 gene reveal the likely genetic basis for epidermolytic hyperkeratosis. *Proc. Natl. Acad. Sci. USA.* 89:6906–6910.

Fujimori, T., and M. Takeichi. 1993. Disruption of epithelial cell–cell adhesion by exogenous expression of a mutated nonfunctional N-cadherin. *Mol. Biol. Cell.* 4:37–47.

Garrod, D.R. 1993. Desmosomes and hemidesmosomes. *Curr. Opin. Cell Biol.* 5:30–40.

Guo, L., Q.-C. Yu, and E. Fuchs. 1993. Targeting expression of keratinocyte growth factor to keratinocytes elicits striking changes in epithelial differentiation in transgenic mice. *EMBO (Eur. Mol. Biol. Organ.) J.* 12:973–986.

Guo, L., L. Degenstein, J. Dowling, Q.-C. Yu, R. Wollmann, B. Perman, and E. Fuchs. 1995. Gene targeting of BPAG1: abnormalities in mechanical strength and cell migration in stratified squamous epithelia and severe neurologic degeneration. *Cell.* 81:233–243.

Hennies, H.C., W. Kuster, D. Mischke, and A. Reis. 1995. Localization of a locus for the striated form of palmoplantar keratoderma to chromosome 18q near the desmosomal cadherin gene cluster. *Hum. Mol. Genet.* 4:1015–1020.

Hermiston, M.L., and J.I. Gordon. 1995. Inflammatory bowel disease and adenomas in mice expressing a dominant negative N-cadherin. *Science (Wash. DC).* 270:1203–1207.

Hodivala, K.J., and F.M. Watt. 1994. Evidence that cadherins play a role in the down-regulation of integrin expression that occurs during keratinocyte terminal differentiation. *J. Cell Biol.* 124:589–600.

Hynes, R.O. 1992. Specificity of cell adhesion in development: the cadherin superfamily. *Curr. Opin. Genet. & Dev.* 2:621–624.

Karpati, S., M. Amagai, R. Prussick, K. Cehrs, and J.R. Stanley. 1993. Pemphigus vulgaris antigen, a desmoglein type of cadherin, is localized within keratinocyte desmosomes. *J. Cell Biol.* 122:409–415.

Kimonis, V., J.J. DiGiovanna, J.M. Yang, S.Z. Doyle, S.J. Bale, and J.G. Compton. 1994. A mutation in the V1 end domain of keratin 1 in non-epidermolytic palmar-plantar keratoderma. *J. Invest. Dermatol.* 103:764–769.

Kintner, C. 1992. Regulation of embryonic cell adhesion by the cadherin cytoplasmic domain. *Cell.* 69:225–236.

Klymkowsky, M.W., and B. Parr. 1995. The body language of cells: the intimate connection between cell adhesion and behavior. *Cell.* 83:5–8.

Koch, P.J., M.J. Walsh, M. Schmeiz, M.D. Goldschmidt, R. Zimbemann, and W.W. Franke. 1990. Desmosomal glycoprotein, as a member of the cadherin family of cell adhesion molecules. *Eur. J. Cell Biol.* 53:1–12.

Kouklis, P., M.E. Hutton, and E. Fuchs. 1994. Making the connection: keratin intermediate filaments and desmosomal proteins. *J. Cell Biol.* 127:1049–1060.

Lever, W.F., and G. Schaumburg-Lever, editors. 1990. Histology of the Skin. 7th ed. J.B. Lippincott Co., Philadelphia. 940 pp.

Levine, E., C.H. Lee, C. Kintner, and B.M. Gumbiner. 1994. Selective disruption of E-cadherin function in early Xenopus embryos by a dominant negative mutant. *Development (Camb.).* 120:901–909.

Mathur, M., L. Goodwin, and P. Cowin. 1994. Interactions of the cytoplasmic domain of the desmosomal cadherin Dsg1 with plakoglobin. *J. Biol. Chem.* 269:14075–14080.

Nagafuchi, A., and M. Takeichi. 1988. Cell binding function of E-cadherin is regulated by the cytoplasmic domain. *EMBO (Eur. Mol. Biol. Organ.) J.* 7:3679–3684.

Nickoloff, B.J., and Y. Naidu. 1994. Perturbation of epidermal barrier function correlates with initiation of cytokine cascade in human skin. *J. Am. Acad. Dermatol.* 30:535–546.

Ozawa, M., and R. Kemler. 1992. Molecular organization of the uvomorulin–catenin complex. *J. Cell Biol.* 116:989–996.

Pasdar, M., and W.J. Nelson. 1988. Kinetics of desmosome assembly in Madin-Darby canine kidney epithelial cells: temporal and spatial regulation of desmoplakin organization and stabilization upon cell–cell contact. II. Morphological analysis. *J. Cell Biol.* 106:687–695.

Pasdar M., K.A. Krzeminski, and W.J. Nelson. 1991. Regulation of desmosome assembly in MDCK epithelial cells: coordination of membrane core and cytoplasmic plaque domain assembly at the plasma membrane. *J. Cell Biol.* 113:645–655.

Potten, C.S. 1981. Cell replacement in epidermis (keratopoiesis) via discrete units of proliferation. *Int. Rev. Cytol.* 69:271–318.

Rheinwald, J.G., and H. Green. 1975. Serial cultivation of strains of human epidermal keratinocytes: the formation of keratinizing colonies from single cells. *Cell.* 6:331–343.

Roh, J.Y., and J.R. Stanley. 1995. Plakoglobin binding by human Dsg3 (pemphigus vulgaris antigen) in keratinocytes requires the cadherin-like intracytoplasmic segment. *J. Invest. Dermatol.* 104:720–724.

Sacco, P.A., T.M. McGranahan, M.J. Wheelock, and K.R. Johnson. 1995. Identification of plakoglobin domains required for association with N-cadherin and alpha-catenin. *J. Biol. Chem.* 270:20201–20206.

Schafer, S., P.J. Koch, and W.W. Franke. 1994. Identification of the ubiquitous human desmoglein, Dsg2, and the expression catalogue of the desmoglein subfamily of desmosomal cadherins. *Exp. Cell Res.* 211:391–399.

Schmelz, M., R. Duden, P. Cowin, and W.W. Franke. 1986. A constitutive transmembrane glycoprotein of M_r 165,000 (desmoglein) in epidermal and non-epidermal desmosomes. I. Biochemical identification of the polypeptide. *Eur. J. Cell Biol.* 42:177–183.

Schmelz, M., R. Moll, C. Kuhn, and W.W. Franke. 1994. Complexus adhaerentes, a new group of desmoplakin-containing junctions in endothelial cells: II. Different types of lymphatic vessels. *Differentiation.* 57:97–117.

Schmidt, A., H.W. Heid, S. Schafer, U.A. Nuber, R. Zimbelmann, and W.W. Franke. 1994. Desmosomes and cytoskeletal architecture in epithelial differentiation: cell type-specific plaque components and intermediate filament anchorage. *Eur. J. Cell Biol.* 65:229–245.

Shimizu, H., T. Masunaga, A. Ishiko, A. Kikuchi, T. Hashimoto, and T. Nishikawa. 1995. Pemphigus vulgaris and pemphigus foliaceus sera show an inversely graded binding pattern to extracellular regions of desmosomes in different layers of human epidermis. *J. Invest. Dermatol.* 105:153–159.

Stanley, J.R. 1993. Cell adhesion molecules as targets of autoantibodies in pemphigus and pemphigoid, bullous diseases due to defective epidermal cell adhesion. *Adv. Immunol.* 53:291–325.

Stoler, A., R. Kopan, M. Duvic, and E. Fuchs. 1988. The use of monospecific antibodies and cRNA probes reveals abnormal pathways of terminal differentiation in human epidermal diseases. *J. Cell Biol.* 107:427–446.

Sun, T.-T., R. Eichner, A. Schermer, D. Cooper, W.G. Nelson, and R.A. Weiss. 1984. The transformed phenotype. *In* The Cancer Cell. Vol. 1. A. Levine, W. Topp, G. van de Woude, and J.D. Watson, editors. Cold Spring Harbor Laboratory, Cold Spring Harbor, NY. 169–176.

Takeichi, M. 1993. Cadherins in cancer: implications for invasion and metastasis. *Curr. Opin. Cell Biol.* 5:806–811.

Troyanovsky, S.M., L.G. Eshkind, R.B. Troyanovsky, R.E. Leube, and W.W. Franke. 1993. Contributions of cytoplasmic domains of desmosomal cadherins to desmosome assembly and intermediate filament anchorage. *Cell.* 72:561–574.

Troyanovsky, S.M., R.B. Troyanovsky, L.G. Eshkind, V.A. Krutovskikh, R.E. Leube, and W.W. Franke. 1994. Identification of the plakoglobin-binding domain in desmoglein and its role in plaque assembly and intermediate filament anchorage. *J. Cell Biol.* 127:151–160.

Vassar, R., M. Rosenberg, S. Ross, A. Tyner, and E. Fuchs. 1989. Tissue-specific and differentiation-specific expression of a human K14 keratin gene in transgenic mice. *Proc. Natl. Acad. Sci. USA.* 86:1563–1567.